

# Extrapolation versus impulse in multiple-timestepping schemes. II. Linear analysis and applications to Newtonian and Langevin dynamics

Eric Barth<sup>a)</sup> and Tamar Schlick<sup>b)</sup>

*Department of Chemistry and Courant Institute of Mathematical Sciences, New York University and Howard Hughes Medical Institute, 251 Mercer Street, New York, New York 10012*

(Received 22 July 1997; accepted 17 February 1998)

Force splitting or multiple timestep (MTS) methods are effective techniques that accelerate biomolecular dynamics simulations by updating the fast and slow forces at different frequencies. Since simple *extrapolation* formulas for incorporating the slow forces into the discretization produced notable energy drifts, symplectic MTS variants based on periodic *impulses* became more popular. However, the efficiency gain possible with these impulse approaches is limited by a timestep barrier due to resonance—a numerical artifact occurring when the timestep is related to the period of the fastest motion present in the dynamics. This limitation is lifted substantially for MTS methods based on extrapolation in combination with stochastic dynamics, as demonstrated for the LN method in the companion paper for protein dynamics. To explain our observations on those complex nonlinear systems, we examine here the stability of extrapolation and impulses to force-splitting in Newtonian and Langevin dynamics. We analyze for a simple linear test system the energy drift of the former and the resonance-related artifacts of the latter technique. We show that two-class impulse methods are generally stable except at integer multiples of half the period of the fastest motion, with the severity of the instability worse at larger timesteps. Extrapolation methods are generally unstable for the Newtonian model problem, but the instability is bounded for increasing timesteps. This boundedness ensures good long-timestep behavior of extrapolation methods for Langevin dynamics with moderate values of the collision parameter. We thus advocate extrapolation methods for efficient integration of the stochastic Langevin equations of motion, as in the LN method described in paper I. © 1998 American Institute of Physics.

[S0021-9606(98)50320-0]

## I. INTRODUCTION

The primary difficulty in computer simulation of large physical systems is efficient treatment of the wide range of temporal and spatial scales present in the underlying models. In the field of biomolecular dynamics, the high-frequency, low-amplitude degrees of freedom dictate a timescale in all-atom models of  $10^{-15}$  s (1 fs). However, large-scale motions of biological interest—such as protein folding—occur on timescales of seconds, many orders of magnitude longer. For a general recent review of methods for biomolecular dynamics, see Ref. 1. Recognizing this formidable range-of-scales problem in simulation and modeling, various timestepping algorithms for numerical dynamics have been introduced. These methods seek to separate spatial scales of the model, treating each at the appropriate temporal scale and combining these levels as accurately and efficiently as possible.

The popular Verlet algorithm<sup>2</sup> is based on a second-order finite-difference discretization of the acceleration in Newton's equations of motion. The method requires calculation of the forces of interaction (the gradient of the potential energy  $E$ , a function of the system coordinates) at each timestep. Effectively, the forces are considered constant dur-

ing each timestep interval. The numerical stability of Verlet depends critically on the period of the fastest motion in the system. This stability requirement limits the timestep size—and hence force recalculation frequency—to the range 0.5 to 1 fs for biomolecular systems modeled with all degrees of freedom flexible. As the system size grows, the number of interactions increases as  $N^2$ , where  $N$  is the number of atoms, and force calculations involving all atom pairs dominate the other operations. Notwithstanding the amount of computational work involved, the Verlet method is often regarded as the “gold standard” for molecular dynamics simulations. The integrator is symplectic,<sup>3</sup> preserving geometric properties (such as time reversibility and phase-space volume) present in the exact solution of these equations for conservative Hamiltonian systems.<sup>3</sup> This preservation likely accounts for the good energy conservation along the computed trajectories observed in practice. This behavior in turn renders the Verlet scheme most suitable for low-accuracy long-time simulations of conservative systems.

Nearly two decades ago, multiple timestep (MTS) methods were introduced<sup>4,5</sup> in an effort to reduce the computational cost of molecular simulations. Assuming that forces due to distant interactions can be held constant to a good approximation over long intervals, ordinary timestepping procedures are modified simply: The long-range forces are evaluated less often than the short-range terms; between updates, these

<sup>a)</sup>Present address: Department of Mathematics, Kalamazoo College, 1200 Academy Street, Kalamazoo, MI 49006.

<sup>b)</sup>Corresponding author; electronic mail: schlick@nyu.edu

slow forces are incorporated into the discretization as constants from step to step. However, this *force extrapolation* approach disrupts the energy-preserving features of the unmodified timestepping algorithms. Therefore, force splitting via extrapolation did not gain wide acceptance in dynamic schemes.

Work continued on MTS methods in a variety of contexts,<sup>6,7</sup> leading to the introduction in 1991 by Grubmüller, Heller, Windemuth, and Schulten<sup>8</sup>—and independently in 1992 by Tuckerman, Berne, and Martyna<sup>9</sup>—of an MTS method which is “Verlet-like” in its energy preservation behavior. This MTS variant, called Verlet-I<sup>8</sup> or r-Respa,<sup>9</sup> establishes a new class of MTS schemes. (The latter is more general.) This class differs from its predecessors in that the forces on each scale are incorporated into the numerical dynamics only at the time of recalculation, with a strength proportional to the interval between evaluations. Thus, as the time interval between slow-force updates increases, the size of these “impulses” grows. Though the original work<sup>8</sup> expressed reservations regarding force impulses, these symplectic MTS variants quickly became favored.

However, recently it has become clear that, like Verlet, considerations of numerical stability also limit the allowable timestep in impulse MTS methods. Namely, rapid energy growth has been observed<sup>10–12</sup> when the interval between slow-force updates approaches and exceeds 5 fs. This barrier, occurring around half the period of the fast motion in biomolecules when all degrees of freedom are allowed (e.g., an O–H bond stretch) can be explained by resonance.<sup>13,14</sup> This resonance refers to an integrator-induced artifact that occurs at particular discretization timesteps related to internal periods of the simulated physical system. See Ref. 13 for a thorough analysis of resonance by the implicit-midpoint scheme and Ref. 14 for a discussion of nonlinear resonance in molecular dynamics.

The presence of these resonances limits the outermost timestep,  $\Delta t$  (i.e., interval of slow-force update), in MTS schemes and thus the overall speedup that can be achieved in practice over a standard Verlet trajectory. When bond lengths are constrained via SHAKE,<sup>15</sup> this artifact is delayed to a timestep related to the light-atom bending modes with period around 20 fs.<sup>16</sup> Other implementational details of the MTS protocol can also delay resonance to larger outer timesteps.

The stability of impulse MTS methods has also been studied for a linear system by García-Archilla, Sanz-Serna, and Skeel.<sup>17</sup> This work offers insight into the nature of instabilities and introduces several “mollified” impulse methods which employ averaging or other smoothing techniques to extend the outer timestep slightly.

In paper I,<sup>18</sup> we introduced an efficient method for biomolecular dynamics that does not suffer from this resonance limitation. Named LN for its origin in a Langevin/Normal-mode scheme,<sup>16,19,20</sup> the method combines force splitting and Langevin dynamics. LN differs from the symplectic MTS schemes Verlet-I<sup>8</sup> and r-Respa<sup>9</sup> in several respects:

(1) The simple Langevin equation is used as the governing equation for dynamics.

- (2) The slow forces are incorporated via extrapolation rather than impulses.
- (3) The short-range motion is propagated on the basis of a linearized model of the equations of motion. This feature of LN, however, can be replaced by direct force calculations;<sup>18</sup> see below.

Results show<sup>18</sup> very good agreement of LN trajectories with small-timestep trajectories for proteins in vacuum and a large water system. The reference simulations used a small timestep of  $\Delta\tau=0.5$  fs, the innermost timestep in LN, as in MTS methods.<sup>11,21</sup> In addition, speedup factors of 10 or more are possible for the larger systems since the outermost timestep ( $\Delta t$ ) can be increased to 48 fs or more.<sup>18</sup>

The success of the LN method in overcoming resonance-related instabilities is the subject of this analytical paper. Among the three distinct features of LN enumerated above, the combination of the two—Langevin heat bath and the extrapolation treatment of the slow forces—allows the use of long timesteps. A Langevin version of Verlet-I<sup>8</sup> and r-Respa<sup>9</sup> at moderate values of the Langevin collision parameter  $\gamma$  appears less sensitive to timesteps near half the fastest period but produces trajectories with exaggerated energies and temperatures for timesteps near that period.<sup>18</sup> Better numerical behavior could be achieved by increasing  $\gamma$  by a factor of 2 or more, but this is undesirable due to substantial damping of the internal modes, especially those of lower frequencies.<sup>18</sup>

In contrast, the LN method is stable at moderate  $\gamma$  across a wide range of outer timesteps, without apparent sensitivity to the periods of fast motion present in the system. As already emphasized, this favorable feature is not a consequence of the linearization treatment of local forces; the replacement of linearization by direct force evaluations results in similar behavior (Barth and Schlick, unpublished data).

In this article we explain these observations on complex nonlinear systems<sup>18</sup> by studying the stability of impulse and extrapolation MTS methods on a simple model problem with two force classes. We emphasize that realistic nonlinear potentials (for proteins) were already tested in paper I; results were so striking that we seek here analytical explanations. Without loss of generality, we formulate impulse and extrapolation MTS methods based on the simple first-order symplectic-Euler method<sup>3</sup> (see paper I<sup>18</sup> for a Verlet-based MTS method). Intermediate techniques described by Scully and Hermans<sup>22</sup> and more recently by Hermans (private communication), developed to correct the effect of constant extrapolation of the slow forces over long timesteps, are also discussed.

We formulate, for each method applied to a simple one-dimensional linear system, the propagation of the dynamics from one timestep to the next as multiplication by a *propagation matrix*. We compute the propagation matrix eigenvalues and examine the relationship between these eigenvalues and the periods of motion in the linear system, outer timestep lengths for the MTS methods, and ultimately the numerical stability of the methods.

This theoretical stability analysis gives insight into the energy drift observed in extrapolation treatments and the timestep barrier associated with impulse methods. We show,

in particular, that extrapolation suffers less dramatically from such a barrier. We then extend the analysis and demonstrate that extrapolation methods are suitable for the efficient simulation of systems modeled by the stochastic Langevin equations of motion. Indeed, these ideas have been successfully applied to the simulation of biomolecular systems by the LN method, presented in paper I.<sup>18</sup>

Although we consider the first-order symplectic-Euler integrator here, our analysis can be easily generalized to Verlet/leapfrog, as well as higher-order methods, and the conclusions are similar. Analogous results with Verlet and further insights into resonance problems will be reported separately.<sup>23</sup>

## II. THE SYMPLECTIC-EULER METHOD AND LINEAR STABILITY

We consider the linear model described by the following system of first-order differential equations:

$$\dot{X} = V, \quad \dot{V} = -(\lambda_1 + \lambda_2)X. \quad (1)$$

The variables  $X$  and  $V$  denote the scalar position and velocity, respectively, for a particle of unit mass. We assume that  $\lambda_2 \ll \lambda_1$  to represent motion components differing in characteristic timescales. The solution of system (1) has the form  $X = \exp(\alpha \pm i\sqrt{\lambda_1 + \lambda_2}t)$ , where  $\alpha$  is a real constant and  $i = \sqrt{-1}$ . Note that the LN method<sup>18</sup> applies force splitting to a linearized system like (1).

We formulate MTS integrators based on the *symplectic-Euler* discretization,<sup>3</sup> given by

$$X^{n+1} = X^n + \Delta\tau V^{n+1}, \quad V^{n+1} = V^n - \Delta\tau\Lambda X^n, \quad (2)$$

where  $\Lambda = \lambda_1 + \lambda_2$  and  $\Delta\tau$  is the timestep. The integer superscript  $n$  refers to the discretized-equation approximation at time  $n\Delta\tau$ .

To establish the methods and notation used later, we examine the stability of the symplectic-Euler method applied to the test system of equation (1). The step-to-step propagation operator  $\Phi: \{V^n, X^n\} \rightarrow \{V^{n+1}, X^{n+1}\}$  can be described by the following matrix equation:

$$\begin{bmatrix} V^{n+1} \\ X^{n+1} \end{bmatrix} = \begin{bmatrix} 1 & 0 \\ \Delta\tau & 1 \end{bmatrix} \begin{bmatrix} 1 & -\Delta\tau\Lambda \\ 0 & 1 \end{bmatrix} \begin{bmatrix} V^n \\ X^n \end{bmatrix}.$$

The  $2 \times 2$  product matrix

$$\mathbf{A}(\Delta\tau, \Lambda) = \begin{bmatrix} 1 & -\Delta\tau\Lambda \\ \Delta\tau & 1 - (\Delta\tau)^2\Lambda \end{bmatrix} = \begin{bmatrix} 1 & 0 \\ \Delta\tau & 1 \end{bmatrix} \begin{bmatrix} 1 & -\Delta\tau\Lambda \\ 0 & 1 \end{bmatrix} \quad (3)$$

defines the method and determines its stability. Namely, the integrator is stable for values of  $\Delta\tau$  and  $\Lambda$  for which the eigenvalues of  $\mathbf{A}$  lie on the closed unit disk in the complex plane. Formally, we say the spectral radius  $\rho(\mathbf{A})$  (the maximum, in absolute value, of the eigenvalues of  $\mathbf{A}$ ) is bounded by unity:  $\rho(\mathbf{A}) \leq 1$ . Here, the eigenvalues of  $\mathbf{A}$  can be computed as

$$1 - \frac{1}{2} \Delta\tau^2\Lambda \pm \frac{1}{4} \sqrt{-4\Delta\tau^2\Lambda + \Delta\tau^4\Lambda^2},$$

or by splitting the expression into real and imaginary parts, as

$$\begin{aligned} & 1 - \frac{1}{2} \Delta\tau^2\Lambda \pm \frac{1}{4} \sqrt{-4\Delta\tau^2\Lambda + \Delta\tau^4\Lambda^2} (1 \\ & \quad + \text{signum}(-4\Delta\tau^2\Lambda + \Delta\tau^4\Lambda^2)) \\ & \pm \frac{1}{4} i \sqrt{-4\Delta\tau^2\Lambda + \Delta\tau^4\Lambda^2} (1 \\ & \quad - \text{signum}(-4\Delta\tau^2\Lambda + \Delta\tau^4\Lambda^2)). \end{aligned}$$

It follows that for  $\Delta\tau$  in the open interval  $(0, 2/\sqrt{\Lambda})$ , the eigenvalues have nonzero imaginary parts, occur in complex conjugate pairs, and are of modulus one—that is, lie on the unit circle in the complex plane. For increasing  $\Delta\tau \geq 2/\sqrt{\Lambda}$ , the eigenvalues are strictly real; one value tends to zero while the other grows without bound. Thus  $\Delta\tau = 2/\sqrt{\Lambda}$  is the maximum stable timestep for the method. This is analogous to the well-known condition for stability of the Verlet method for a harmonic oscillator:  $2/\omega$  or  $P/\pi$ , where  $P$  is the oscillator's period.

The fact that all stable timesteps correspond to propagation matrix eigenvalues with modulus one is related to the structure-preserving properties of the symplectic method.<sup>3</sup> The determinant of this matrix (equal to the product of the two eigenvalues) is one, implying the preservation of volume in phase space. In the one-dimensional system considered here, volume preservation is equivalent to symplecticity.

Figure 1 illustrates the relationship between the propagation matrix eigenvalues and the stability of the symplectic-Euler scheme for  $\Lambda = 400$ . Panel (a) shows the magnitude of both eigenvalues as a function of the timestep  $\Delta\tau$ . This magnitude departs from unity at the timestep  $\Delta\tau = 2/\sqrt{\Lambda} = 0.1$ ; for larger timesteps, one eigenvalue tends to zero and the other grows in magnitude beyond one. The other panels show the complex eigenpairs for selected timesteps represented as vectors. On the unit circle, points correspond to the eigenvalues computed for timesteps  $\Delta\tau = 0.001n$  for integers  $n$  in the range  $\Delta\tau = 0$  to  $\Delta\tau = 0.1$ . We see that the two eigenvalues begin on the real axis at one for  $\Delta\tau = 0$  (b) and, as  $\Delta\tau$  increases, travel as complex conjugate pairs in opposite directions around the unit circle [parts (c)–(e)]. At the stability threshold of  $\Delta\tau = 2/\sqrt{\Lambda}$ , the two eigenvalues converge on the real axis at  $-1$  (f), remaining on the real axis thereafter and departing from the unit circle (g). This behavior—complex eigenvalues converging to a point on the real axis—is associated with instabilities for each of the methods considered in the remainder of the paper.

## III. STABILITY OF IMPULSE AND EXTRAPOLATION TREATMENTS

We now consider the stability of impulse and extrapolation force-splitting methods for Newtonian and Langevin dynamics in turn.

### A. Newtonian dynamics

An impulse MTS method treats the slow component (associated with  $\lambda_2$ ) of the force at timesteps  $k$  times larger than those for the fast ( $\lambda_1$ ) components. A discretization scheme based on system (3) above is

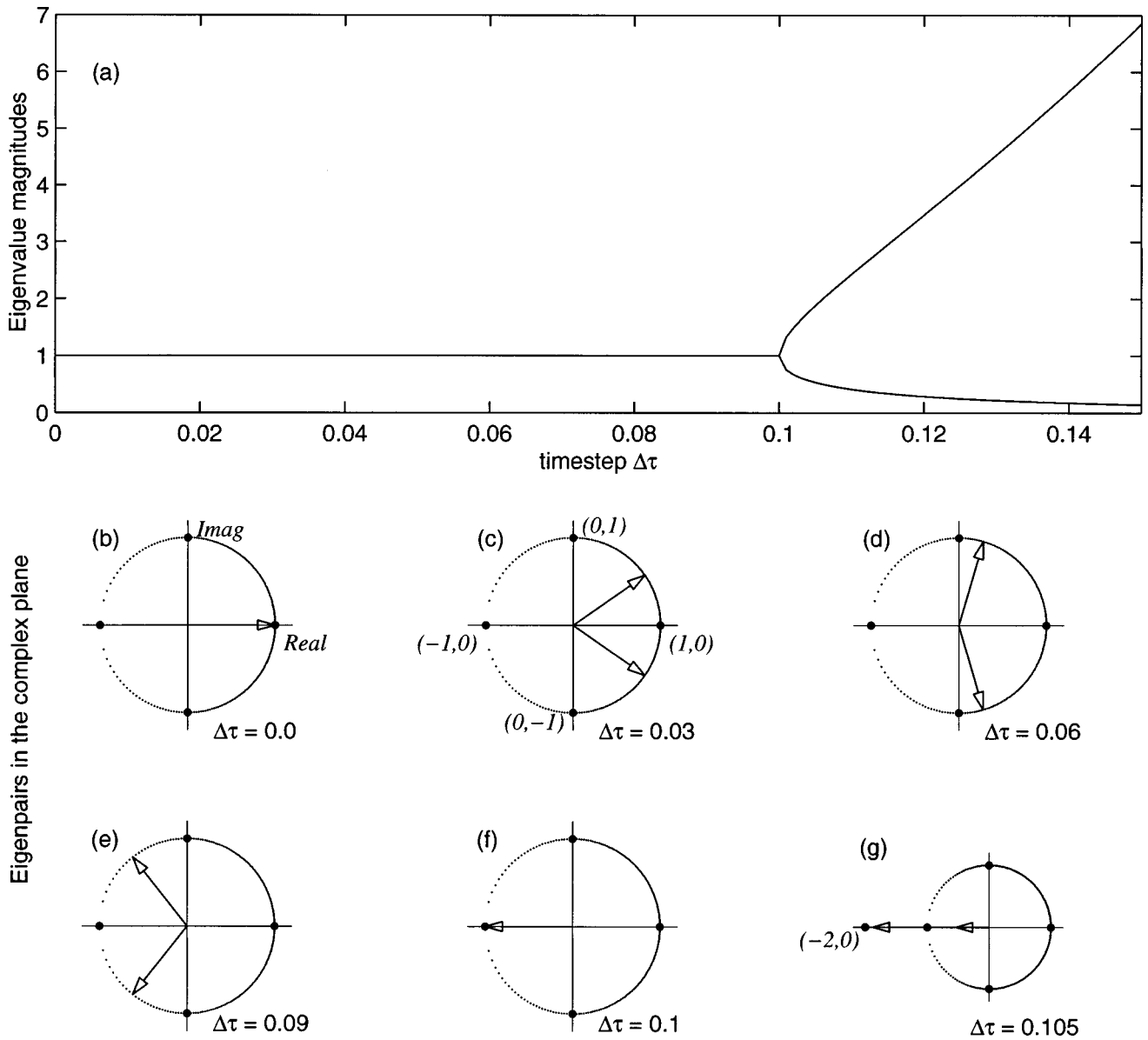


FIG. 1. Propagation-matrix eigenvalue magnitudes for the symplectic-Euler method given by equation (3) applied to the linear test system,  $\Lambda = 400$ , plotted versus the timestep,  $\Delta\tau = 0.001n$  for integers  $n$  [panel (a)], and the two eigenvalues plotted as vectors in the complex plane for selected  $\Delta\tau$  (b)–(g). The method is stable for  $0 \leq \Delta\tau \leq 2/\sqrt{\Lambda} = 0.1$ , and in this interval, the eigenvalues occur in complex conjugate pairs, (b)–(f). For  $\Delta\tau > 2/\sqrt{\Lambda}$ , the eigenvalues of the propagation matrix depart from the unit circle along the real axis (g), one growing without bound and the other approaching zero. On the unit circle in parts (b)–(g), points correspond to eigenpairs for  $\Delta\tau$  equal to integral multiples of 0.001.

**Impulse Method**

$X^0 = X^n$ ,  
 $V^0 = V^n - k\Delta\tau\lambda_2 X^n$   
**for**  $i = 0, k - 1$   
 $V^{i+1} = V^i - \Delta\tau\lambda_1 X^i$ ,  
 $X^{i+1} = X^i + \Delta\tau V^{i+1}$

**end**

$V^{n+1} = V^k$ ,  
 $X^{n+1} = X^k$ .

(The index  $i$  above and hereafter should not be confused with the complex number.) The associated propagation matrix  $\mathbf{A}_I$  for this method is given by

$$\mathbf{A}_I(\Delta\tau, \lambda_1, \lambda_2, k) = \begin{bmatrix} 1 & -\Delta\tau\lambda_1 \\ \Delta\tau & 1 - (\Delta\tau)^2\lambda_1 \end{bmatrix}^k \begin{bmatrix} 1 & -k\Delta\tau\lambda_2 \\ 0 & 1 \end{bmatrix} \quad (4)$$

$$= \mathbf{A}(\Delta\tau, \lambda_1)^k \begin{bmatrix} 1 & -k\Delta\tau\lambda_2 \\ 0 & 1 \end{bmatrix}. \quad (5)$$

It can be shown that the determinant of the matrix  $\mathbf{A}_I$  is always one, just as in the case for symplectic-Euler. Thus, this formulation results in a symplectic method. We shall see, however, that the impulse formulation suffers from resonance-related instabilities at certain timestep lengths. For

timesteps short enough to avoid these instabilities, the structure-preserving properties of this method make it most suitable for Newtonian dynamics.

To avoid the impulses proportional to  $k\Delta\tau$ —and perhaps lessen the effects of resonance-related instabilities—we hold the slow component of the force constant over  $k$  steps. This approach results in the following alternative treatment:

**Extrapolation Method**

$$X^0 = X^n, \\ V^0 = V^n$$

**for**  $i = 0, k-1$

$$V^{i+1} = V^i - \Delta\tau(\lambda_1 X^i + \lambda_2 X^0), \\ X^{i+1} = X^i + \Delta\tau V^{i+1}$$

**end**

$$V^{n+1} = V^k, \\ X^{n+1} = X^k.$$

As before, the slow force ( $\lambda_2 X^0$ ) is evaluated at intervals  $k\Delta\tau$ , but in contrast to the impulse method, this constant force contributes to the numerical dynamics at every inner step  $\Delta\tau$ .

Defining the extrapolation matrix  $\mathbf{E}$  as

$$\mathbf{E}(h, \lambda) = \begin{bmatrix} 0 & -h\lambda \\ 0 & 0 \end{bmatrix},$$

we obtain the relevant propagation matrix  $\mathbf{A}_E$  in terms of  $\mathbf{A}$  above and  $\mathbf{E}$  for a step of length  $k\Delta\tau$  for the extrapolation method:

$$\mathbf{A}_E(\Delta\tau, \lambda_1, \lambda_2, k) = \mathbf{A}(\Delta\tau, \lambda_1)^k + (\mathbf{A}(\Delta\tau, \lambda_1)^k \\ + \mathbf{A}(\Delta\tau, \lambda_1)^{(k-1)} + \dots \\ + \mathbf{A}(\Delta\tau, \lambda_1))\mathbf{E}(\Delta\tau, \lambda_2). \quad (6)$$

In Figure 2 we illustrate behavior of the impulse and extrapolation variants of the symplectic-Euler scheme for the case of  $\lambda_1 = 400$  and  $\lambda_2 = 1$ . In the central panel, we show the eigenvalue magnitudes of the associated propagation matrices— $\mathbf{A}_I$  and  $\mathbf{A}_E$ , respectively—as a function of the timestep. The period associated with each exponential component of the solution,  $e^{i\sqrt{\lambda}t}$ , is  $P = 2\pi/\sqrt{\lambda}$ . Hence for  $\lambda_1 = 400$ , the period  $P_1 \approx 0.314$  in our units, and for  $\lambda_2 = 1$ ,  $P_2 = 2\pi$ , 20 times larger.

For the results in Figure 2, we use  $\Delta\tau = 0.001$  (the inner timestep) and  $k\Delta\tau$  for the outer timestep. The maximum outer timestep shown (unity) corresponds to about three times the period of the fast motion. We see from the figure that the impulse method is unstable at certain timesteps—integral multiples of half the fastest period. The severity of these corruptions increases with  $k$ , approximately as  $e^{\pm\lambda_2 k \Delta\tau / (2\sqrt{\lambda_1})}$ . This can be seen from the lower panel of Figure 2, which extends the middle view to larger outer timesteps approaching the period of the slow motion ( $2\pi$ ). Impulses clearly lead to serious artifacts at certain timesteps. For other timesteps, however, the impulse method is stable—the eigenvalues have magnitude one. Still, for a large nonlinear system, it is likely that once a resonant timestep is reached, good numerical behavior cannot be reestablished by increasing the timestep.<sup>14</sup> That is, avoiding resonant timesteps is virtually impossible due to many clustered vibrational modes and intricate coupling between them.

For the extrapolation method, in contrast, we note deviations from unit eigenvalues except at integral multiples of the fast period. Since both eigenvalues exceed one in magnitude, the determinant of  $\mathbf{A}_E$  is also greater than one, implying that the method is not volume-preserving or symplectic. This explains the energy drift observed in practice for such methods. The sinusoidal pattern of the extrapolation plot has amplitude  $\lambda_2/\lambda_1$  (0.0025 here); therefore, the larger the separation of frequencies, the more benign the numerical artifacts in practice.

At half-period multiples, spikes are also seen for the extrapolation method, but they do not increase in magnitude as  $k$  increases. The upper magnified views of Figure 2 show, for the extrapolation and impulse methods, the spikes in detail for  $k\Delta\tau$  near  $\frac{1}{2}$ ,  $\frac{3}{2}$ , and  $\frac{5}{2}$  the period associated with  $\lambda_1$ . This boundedness associated with the extrapolation approach, together with the discussion in the next section, explains the good behavior of LN at large timesteps observed in practice.<sup>18</sup>

Interestingly, a method which lies between these two force-splitting extremes was proposed by Scully and Hermans,<sup>22</sup> and recently modified Hermans [J. Hermans (private communication)]. These extrapolative/correction methods seek to improve the behavior of the low-order extrapolation by introducing corrections to the velocity (and in the original method to the position as well) after extrapolation:

**Extrapolation/Correction Methods**

$$V^0 = V^n, \\ X^0 = X^n$$

**for**  $i = 0, k-1$

$$V^{i+1} = V^i - \Delta\tau(\lambda_1 X^i + \lambda_2 X^0), \\ X^{i+1} = X^i + \Delta\tau V^{i+1}$$

**end**

$$V^{n+1} = V^k - \frac{k-1}{2} \Delta\tau(\lambda_2 X^k - \lambda_2 X^0),$$

$$X^{n+1} = X^k - \left[ \frac{k^2-1}{6} (\Delta\tau)^2 (\lambda_2 X^k - \lambda_2 X^0) \right].$$

Omission of the position correction (enclosed by square brackets in the last line above), constitutes the recent modification, resulting in a scheme we call the Extrapolate/Correct<sub>v</sub> method. The propagation matrix associated with this method is

$$\mathbf{A}_{E/C_v}(\Delta\tau, \lambda_1, \lambda_2, k) = \left( \mathbf{I} + \mathbf{E} \left( \frac{k-1}{2} \Delta\tau, \lambda_2 \right) \right) \\ \times \mathbf{A}_E(\Delta\tau, \lambda_1, \lambda_2, k) - \mathbf{E} \left( \frac{k-1}{2} \Delta\tau, \lambda_2 \right). \quad (7)$$

To express the propagation matrix for the Extrapolate/Correct<sub>v,x</sub> method, we first introduce the following extrapolation matrix:

$$\mathbf{E}_X(h, \lambda) = \begin{bmatrix} 0 & 0 \\ 0 & -h\lambda \end{bmatrix}.$$

Then the propagation matrix for this method can be expressed as

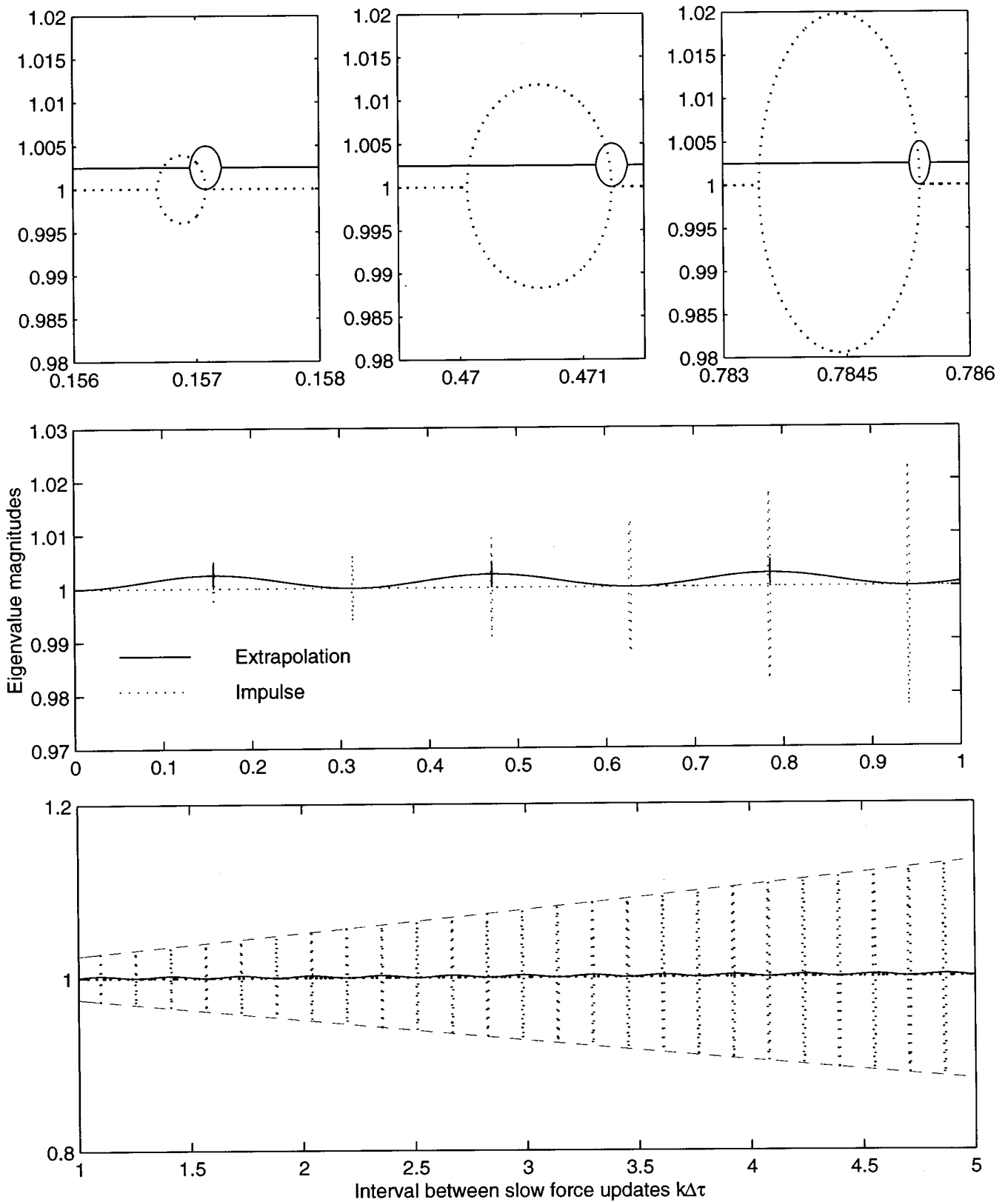


FIG. 2. Propagation-matrix eigenvalue magnitudes for the impulse method given by equation (5) ( $\cdots$ ) applied to the linear test system,  $\lambda_1=400$ ,  $\lambda_2=1$ , versus the extrapolation method of equation (6) ( $-$ ), plotted as a function of the outer timestep. The upper magnified views show the behavior near odd multiples of the period associated with  $\lambda_1$ . The lower view extends the outer timestep near the period ( $2\pi$ ) of the motion due to the slow force. The spikes associated with the impulse method grow with increasing  $k$  like  $\exp\{\pm(\lambda_2 k \Delta\tau) / (2\sqrt{\lambda_1})\}$  ( $- -$ ).

$$\begin{aligned} \mathbf{A}_{E/C_{V,X}}(\Delta\tau, \lambda_1, \lambda_2, k) = & \left( \mathbf{I} + \mathbf{E} \left( \frac{k-1}{2} \Delta\tau, \lambda_2 \right) \right. \\ & \left. + \mathbf{E}_X \left( \frac{k^2-1}{6} (\Delta\tau)^2, \lambda_2 \right) \right) \mathbf{A}_E(\Delta\tau, \lambda_1, \lambda_2, k) \\ & - \mathbf{E} \left( \frac{k-1}{2} \Delta\tau, \lambda_2 \right) - \mathbf{E}_X \left( \frac{k^2-1}{6} (\Delta\tau)^2, \lambda_2 \right). \end{aligned} \quad (8)$$

Behavior of these two methods for our model problem can be seen in Figure 3. The magnified inset shows small deviation from unit eigenvalues for  $k\Delta\tau$  less than about one quarter the period of the fast motion. This result likely explains the good behavior in practice for the methods at moderate timesteps, as well as the slight energy damping (associated with eigenvalues less than unity) for the original extrapolation/correction method [J. Hermans (private communication)]. At large timesteps, however, both schemes suffer from sinusoidal oscillations with increasing amplitude, as well as spikes at multiples of half the period; these spikes grow in height with increasing  $k$ .

### B. Langevin dynamics

The stochastic Langevin framework has been used as the underlying dynamical model in a number of molecular modeling contexts,<sup>24–32</sup> as well as a stabilizing influence from a numerical point of view.<sup>16,19,20,33</sup> With this in mind, we now extend the stability discussions above to Langevin dynamics.

We consider the Langevin equations of motion

$$\dot{X} = V, \quad \dot{V} = -(\lambda_1 + \lambda_2)X - \gamma V + R, \quad (9)$$

with the friction parameter  $\gamma$ . The random force  $R$  is a stationary Gaussian process with statistical properties given by

$$\langle R(t) \rangle = 0, \quad \langle R(t)R(t') \rangle = 2\gamma k_B T M \delta(t-t'),$$

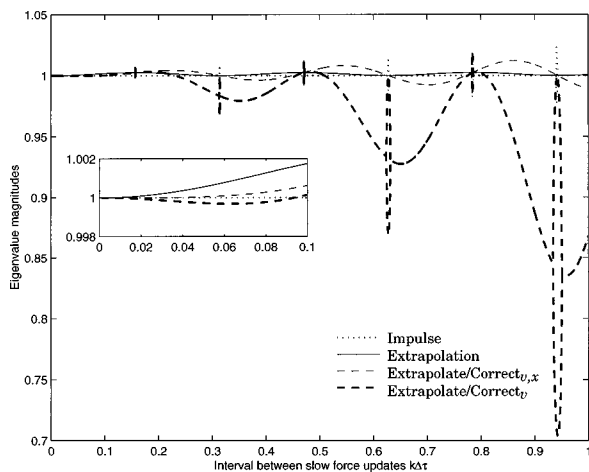


FIG. 3. Propagation-matrix eigenvalue magnitudes for the extrapolation/correction methods of equation (8) (—) and equation (7) (---). Eigenvalue magnitudes for the impulse (···) and pure extrapolation (—) MTS methods are included for comparison.

where  $T$  is the temperature,  $k_B$  is Boltzmann's constant, and  $\delta$  is the Dirac  $\delta$ -function. As before, we assume a unit mass matrix  $\mathbf{M}$ .

The symplectic-Euler method applied to this equation becomes

$$\begin{aligned} X^{n+1} &= X^n + \Delta\tau V^{n+1}, \\ V^{n+1} &= (1 - \gamma\Delta\tau)V^n - \Delta\tau\Lambda X^n + \Delta\tau R^n, \end{aligned} \quad (10)$$

where again  $\Lambda = \lambda_1 + \lambda_2$ . The corresponding step-to-step propagation can be described compactly as

$$\begin{bmatrix} V^{n+1} \\ X^{n+1} \end{bmatrix} = \begin{bmatrix} 1 - \Delta\tau\gamma & -\Delta\tau\Lambda \\ \Delta\tau(1 - \Delta\tau\gamma) & 1 - (\Delta\tau)^2\Lambda \end{bmatrix} \begin{bmatrix} V^n \\ X^n \end{bmatrix} + \begin{bmatrix} \Delta\tau R \\ \Delta\tau^2 R \end{bmatrix}. \quad (11)$$

This expression resembles those given in equations (5) and (6)—a multiplication of the vector  $[V^n, X^n]^T$  by a matrix with entries involving  $X, V, \Lambda, k, \Delta\tau$ , and  $\gamma$ . It differs from those deterministic formulations in the addition of a vector of random variables not dependent on  $\Lambda, X$ , and  $V$ . We follow Kloeden and Platen<sup>34</sup> in examining the method's stability independent of the random vector, and define the stability matrix for the Langevin integrator as the propagation matrix for a damped oscillator with linear friction coefficient  $\gamma$ :

$$\mathbf{A}^{\mathcal{L}}(\Delta\tau, \Lambda, \gamma) = \begin{bmatrix} 1 - \Delta\tau\gamma & -\Delta\tau\Lambda \\ \Delta\tau(1 - \Delta\tau\gamma) & 1 - (\Delta\tau)^2\Lambda \end{bmatrix}. \quad (12)$$

Here the superscript  $\mathcal{L}$  denotes the generalization to Langevin dynamics of the stability matrix  $\mathbf{A}$  defined in equation (3). As before, the method is stable at values of  $\Delta\tau, \Lambda$ , and  $\gamma$  for which the spectral radius is bounded by unity.

Similarly, the stability of the impulse and extrapolation MTS methods applied to the Langevin equations (9) is determined by the eigenvalues of the matrices

$$\mathbf{A}_I^{\mathcal{L}}(\Delta\tau, \lambda_1, \lambda_2, k, \gamma) = \mathbf{A}^{\mathcal{L}}(\Delta\tau, \lambda_1, \gamma)^k \begin{bmatrix} 1 & -k\Delta\tau\lambda_2 \\ 0 & 1 \end{bmatrix} \quad (13)$$

and

$$\begin{aligned} \mathbf{A}_E^{\mathcal{L}}(\Delta\tau, \lambda_1, \lambda_2, k, \gamma) &= \mathbf{A}^{\mathcal{L}}(\Delta\tau, \lambda_1, \gamma)^k \\ &+ (\mathbf{A}^{\mathcal{L}}(\Delta\tau, \lambda_1, \gamma))^k \\ &+ \mathbf{A}^{\mathcal{L}}(\Delta\tau, \lambda_1, \gamma)^{(k-1)} + \dots \\ &+ \mathbf{A}^{\mathcal{L}}(\Delta\tau, \lambda_1, \gamma) \mathbf{E}(\Delta\tau, \lambda_2). \end{aligned} \quad (14)$$

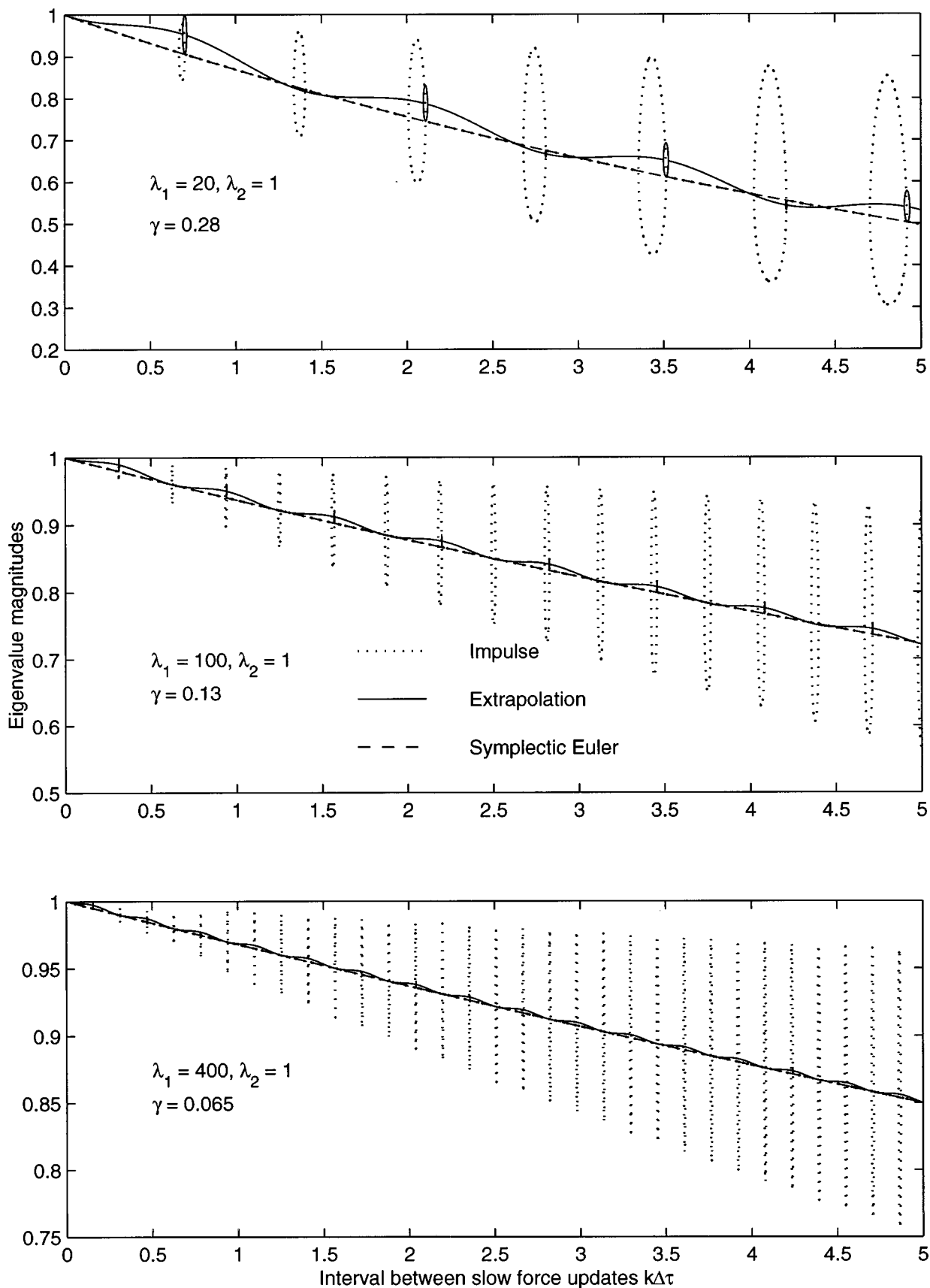


FIG. 4. Propagation-matrix eigenvalue magnitudes for the symplectic-Euler method given by equation (12) (---), the impulse MTS method of equation (13) (···), and the extrapolation method of equation (14) (—) applied to the Langevin linear test system for  $\lambda_2=1$  with  $\lambda_1=20, 100,$  and  $400$ . The Langevin parameter  $\gamma$  in each case is the minimal stable value for the extrapolation method, computed by the formula in equation (15). For the symplectic-Euler method, the notion of outer timestep  $k\Delta\tau$  reduces to applying  $k$  steps of the method defined by equation (14) with timestep  $\Delta\tau$ .



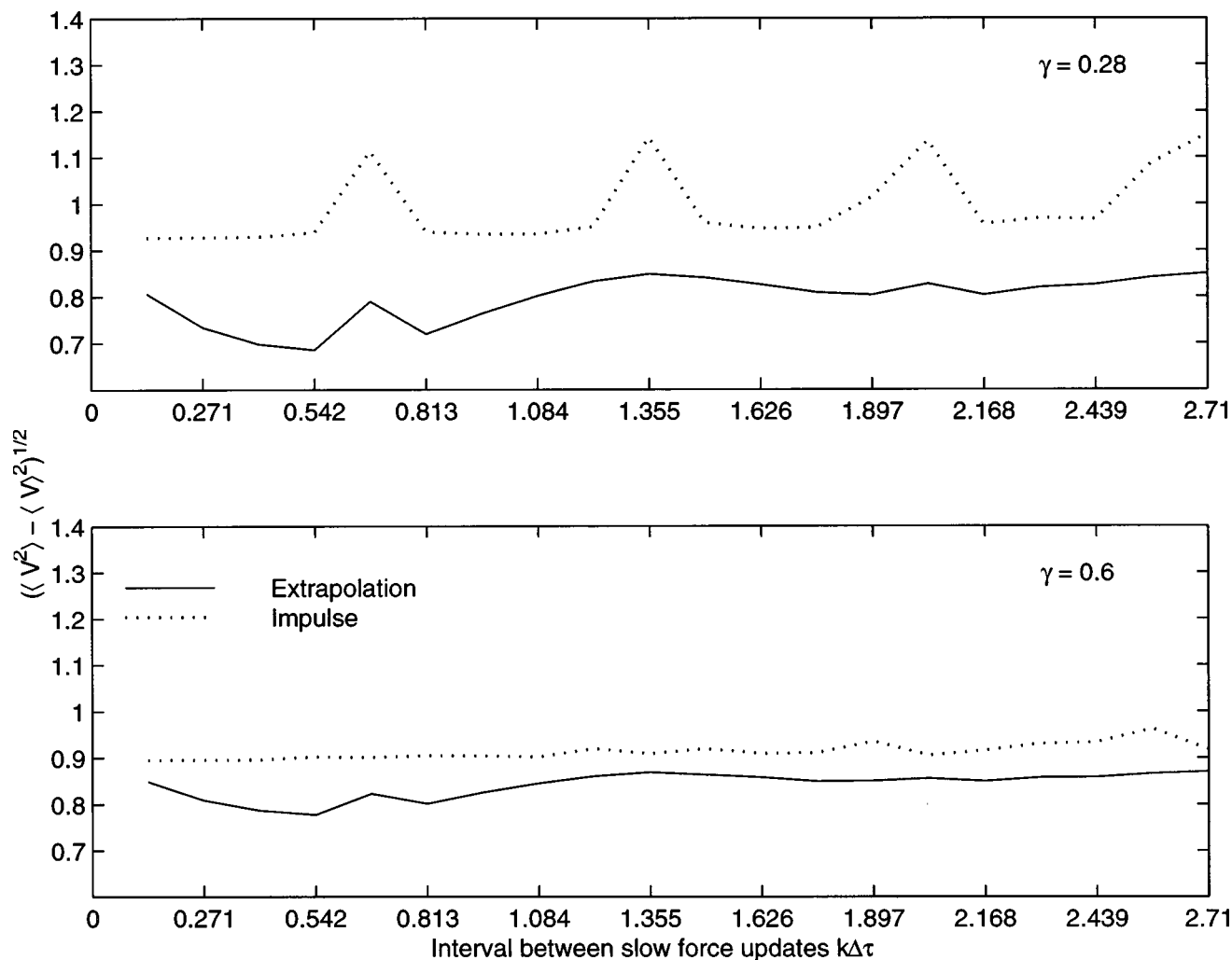


FIG. 5. Root-mean-square fluctuations of the velocity over 3000 steps of integration of the Langevin linear test system by the impulse ( $\cdots$ ) and extrapolation ( $—$ ) MTS treatments with  $\lambda_1=20$ ,  $\lambda_2=1$ . The upper view, corresponding to Langevin parameter  $\gamma=0.28$ , shows resonance effects in the impulse method. A larger  $\gamma$  is required to eliminate this behavior (bottom view).

We have already observed in Figure 2 that the oscillation in the propagation matrix eigenvalues for the extrapolation method has amplitude  $\lambda_2/\lambda_1$  (with a peak of  $1+2\lambda_2/\lambda_1$  at odd multiples of half the fast period) and approximately the same period as the motion associated with  $\lambda_1$ , ( $P=2\pi/\sqrt{\lambda_1}$ ). The spectral radius of the exact flow of the damped oscillator should decay (due to friction) like  $e^{-\gamma t/2}$ . Thus for a given value of  $\gamma$ , the exponentially decaying eigenvalue oscillations should be bounded above, for all  $\Delta t$ , by

$$\exp\{-(\gamma\Delta t)/2\}[1+(2\lambda_2)/\lambda_1].$$

Substituting half the period of the fastest motion for  $\Delta t$ , and requiring the eigenvalue magnitudes to be restricted to unity or less, we have

$$1 \geq \exp\{-(\gamma\pi)/(2\sqrt{\lambda_1})\}[1+(2\lambda_2)/\lambda_1].$$

We next solve the inequality for  $\gamma$ :

$$\gamma \geq (2\sqrt{\lambda_1})/\pi \ln[1+(2\lambda_2)/\lambda_1], \quad (15)$$

to obtain the minimum value  $\gamma$  which assures stability of the extrapolation method at all outer timesteps  $\Delta t=k\Delta\tau$ .

Figure 4 shows eigenvalue magnitudes for the two schemes for  $\lambda_2=1$  and three ratios:  $\lambda_1/\lambda_2=20,100,400$  (or a period ratio of 20, 10, and  $\sqrt{20}$ , respectively). The  $\gamma$  values 0.28, 0.13 and 0.065 in Figure 4 were calculated in each case from formula (15).

The eigenvalue magnitudes decrease with the outer timestep. In Langevin dynamics, this effect is compensated by the restoring force  $R$  in equation (9). The greater rate of damping for larger  $\gamma$ , as is physically correct, is evident (note the different lower ordinate value in each  $\gamma$  panel). The figure also suggests that instability results when  $\gamma$  is too small. This has been observed for the LN method.<sup>18</sup> The dependency on the ratio  $\lambda_1/\lambda_2$  emerges from the other parts of the figure.

Figure 4 further shows that the Langevin/impulse approach is stable for the chosen  $\gamma$ , since the eigenvalues do not exceed unity in magnitude. However, the large deviations from the damped oscillator spectral radius of  $e^{-\gamma t/2}$  can result in stable, but incorrect Langevin trajectories. This is demonstrated in Figure 5, where the root-mean-square fluctuations in velocity are plotted versus the outer timestep for

two values of  $\gamma$ . We see that a larger value of  $\gamma$  is required by the impulse method than by extrapolation. This behavior has been noted in practice in paper I<sup>18</sup> for a protein and a water system; namely, a Langevin/impulse MTS method at outer timestep near the period of the fastest motion produces trajectories with erroneously high energy and temperature averages at moderate values of  $\gamma$ . This artifact can only be remedied by increasing  $\gamma$  by more than a factor of 2.

#### IV. SUMMARY AND CONCLUSIONS

We have analyzed, for a simple linear test system, the behavior of impulse and extrapolative dual-timestep approaches. It is clear that impulse treatments lead to resonances, or corrupted behavior, at outer timesteps which are related to multiples of half the period associated with the fastest motion, even though the inner timestep remains small. This limits the speedup gains in symplectic MTS versions used for biomolecular dynamics to factors around five.<sup>11,21</sup> The extrapolation treatment does not suffer from these dramatic effects, but reveals mild sinusoidal departures from structure-preserving properties. Hence, we suggest that extrapolative treatments are most suitable for long timesteps in the context of Langevin dynamics, where the damping and stochastic terms exert a stabilizing influence. Moreover, the additional terms of the Langevin equation can be small, just sufficient for stability. We have used  $\gamma$  in the range 10–20 ps<sup>-1</sup> in LN for good numerical behavior, as well as good agreement with Newtonian dynamics.<sup>1,18</sup> Recently suggested<sup>22</sup> hybrids of impulse and extrapolation techniques slightly improve numerical behavior of extrapolation methods at small timesteps but exhibit serious instabilities which grow with increasing timestep.

Clearly, our results can be generalized to more complicated reference integration schemes,<sup>23</sup> to more than two timestep classes (where resonance is likely delayed to a larger outer timestep), and possibly to simple nonlinear systems. Still, the linear test cases analyzed here already suggest the basic guidelines we seek. Behavior in practice for multiscale nonlinear systems can only be tested by computer simulations proper.

#### ACKNOWLEDGMENTS

Support from the National Institutes of Health and the National Science Foundation is gratefully acknowledged. We thank Jan Hermans for valuable scientific exchanges related to multiple-timestep variants. T.S. is an investigator of the Howard Hughes Medical Institute.

- <sup>1</sup>T. Schlick, E. Barth, and M. Mandziuk, *Annu. Rev. Biophys. Biomol. Struct.* **26**, 179 (1997).
- <sup>2</sup>L. Verlet, *Phys. Rev.* **159**, 98 (1967).
- <sup>3</sup>J. M. Sanz-Serna and M. P. Calvo, *Numerical Hamiltonian Problems* (Chapman and Hall, London, 1994).
- <sup>4</sup>W. B. Streett, D. J. Tildesley, and G. Saville, *Mol. Phys.* **35**, 639 (1978).
- <sup>5</sup>R. D. Swindoll and J. M. Haile, *J. Chem. Phys.* **53**, 289 (1984).
- <sup>6</sup>M. E. Tuckerman, B. J. Berne, and A. Rossi, *J. Chem. Phys.* **94**, 1465 (1991).
- <sup>7</sup>M. E. Tuckerman and B. J. Berne, *J. Comput. Chem.* **95**, 8362 (1992).
- <sup>8</sup>H. Grubmüller, H. Heller, A. Windemuth, and K. Schulten, *Mol. Simul.* **6**, 121 (1991).
- <sup>9</sup>M. E. Tuckerman, B. J. Berne, and G. J. Martyna, *J. Chem. Phys.* **97**, 1990 (1992).
- <sup>10</sup>R. Zhou and B. J. Berne, *J. Chem. Phys.* **103**, 9444 (1995).
- <sup>11</sup>M. Watanabe and M. Karplus, *J. Phys. Chem.* **99**, 5680 (1995).
- <sup>12</sup>T. Bishop, R. D. Skeel, and K. Schulten, *J. Comput. Chem.* **18**, 1785 (1997).
- <sup>13</sup>M. Mandziuk and T. Schlick, *Chem. Phys. Lett.* **237**, 525 (1995).
- <sup>14</sup>T. Schlick, M. Mandziuk, R. D. Skeel, and K. Srinivas, *J. Comput. Phys.* **139**, 1 (1998).
- <sup>15</sup>J. P. Ryckaert, G. Ciccotti, and H. J. C. Berendsen, *J. Comput. Phys.* **23**, 327 (1977).
- <sup>16</sup>E. Barth, M. Mandziuk, and T. Schlick, in *Computer Simulation of Biomolecular Systems: Theoretical and Experimental Applications*, edited by W. F. van Gunsteren, P. K. Weiner, and A. J. Wilkinson, Vol. III, Chap. 4 (ESCOM, Leiden, The Netherlands, 1997), pp. 97–121.
- <sup>17</sup>B. García-Archilla, J. M. Sanz-Serna, and R. D. Skeel, *SIAM J. Sci. Comp.* (to appear); Also Tech. Rept. 1996/7, Dep. Math. Applic. Comput., Univ. Valladolid, Valladolid, Spain.
- <sup>18</sup>E. Barth and T. Schlick, *J. Chem. Phys.* **109**, 1617 (1998).
- <sup>19</sup>G. Zhang and T. Schlick, *J. Comput. Chem.* **14**, 1212 (1993).
- <sup>20</sup>G. Zhang and T. Schlick, *J. Chem. Phys.* **101**, 4995 (1994).
- <sup>21</sup>D. E. Humphreys, R. A. Friesner, and B. J. Berne, *J. Phys. Chem.* **98**, 6885 (1994).
- <sup>22</sup>J. L. Scully and J. Hermans, *Mol. Simul.* **11**, 67 (1993).
- <sup>23</sup>A. Sandu and T. Schlick (in preparation).
- <sup>24</sup>R. W. Pastor, in *The Molecular Dynamics of Liquid Crystals*, edited by G. R. Luckhurst and C. A. Veracini (Kluwer Academic, Dordrecht, The Netherlands, 1994), pp. 85–138.
- <sup>25</sup>R. J. Loncharich, B. R. Brooks, and R. W. Pastor, *Biopolymers* **32**, 523 (1992).
- <sup>26</sup>P. Derreumaux and T. Schlick, *Proteins: Struct., Funct., Genet.* **21**, 282 (1995).
- <sup>27</sup>M. H. Hao, M. R. Pincus, S. Rackovsky, and H. A. Scheraga, *Biochemistry* **32**, 9614 (1993).
- <sup>28</sup>A. Brünger, C. L. Brooks III, and M. Karplus, *Chem. Phys. Lett.* **105**, 495 (1982).
- <sup>29</sup>T. Simonson, *Chem. Phys. Lett.* **250**, 450 (1996).
- <sup>30</sup>D. Beglov and B. Roux, *J. Chem. Phys.* **100**, 9050 (1994).
- <sup>31</sup>D. Beglov and B. Roux, *Biopolymers* **35**, 171 (1994).
- <sup>32</sup>D. Beglov and B. Roux, *J. Chem. Phys.* **103**, 360 (1995).
- <sup>33</sup>C. S. Peskin and T. Schlick, *Commun. Pure Appl. Math.* **42**, 1001 (1989).
- <sup>34</sup>P. E. Kloeden and E. Platen, *J. Stat. Phys.* **66**, 283 (1992).